Statistical model of the impulse response of a reverberant plate : application to parameter estimation and correlation analysis

Emmanuel Moulin, Hossep Achdjian, Jamal Assaad, Farouk Benmeddour, Karl Hourany, Youssef Zaatar

ACOUSTICS 2012

Statistical model of the impulse response of a reverberant plate: application to parameter estimation and correlation analysis

E. Moulin[a], H. Achdjian[a], J. Assaad[a], F. Benmeddour[a], K. Hourany[b] and Y. Zaatar[b]

[a]IEMN, Le Mont Houy, F-59313 Valenciennes, France
[b]Université Libanaise,
emmanuel.moulin@univ-valenciennes.fr

The acoustic reverberation in a solid plate can be conveniently modeled through a nonstationary random process based on the image-sources method. The interest of such a statistical model is to allow the prediction of a general behaviour (in the form of mathematical expectations) from a limited set of experimentally accessible parameters. Contrary to previous works, the model presented here takes into account the dispersive nature of plate waves (Lamb waves). Then, the relations between the average signal envelopes or correlation functions and the reverberation properties of the medium and the relative positions of the noise source, the sensor(s) and, possibly, the defect are derived. Two kinds of possible applications of these theoretical results will be illustrated: (1) parameter extraction such as source-receiver distance, structural dimensions or propagation velocities through curve-fitting; (2) imaging potentialities from ambient acoustic noise correlation.

1 Introduction

Multi-path acoustic propagation inside a closed medium contains potentially useful information about the structural properties of the medium. Means of extracting this information are currently the subject of intense research work. Powerful techniques such as time-reversal acoustics [1, 2], field correlation [3, 4, 5, 6], or diffusing acoustic wave spectroscopy [7, 8] all belong to this context.

In highly reverberant media, the low acoustic attenuation and the multiple reflections should allow both a full-scale exploration of the structural properties and a high sensitivity to the presence of a defect.

In this paper we present a time-domain statistical description, relying on a shot-noise assumption, well suited to predict the average characteristics of dispersive signals received at localised points of a reverberant medium. The basis of this model is the image-source method [9, 10], that is used to estimate the average wavepacket distributions in the signals.

First the useful theoretical relationships are derived from the statistical model. Theoretical expressions for the mathematical expectations of the squared envelopes and the squared correlation functions of signals received after reverberant dispersive propagation in the medium are obtained. Then, interesting and original possible applications of these relationships to parameter estimation and defect detection capabilities are demonstrated.

2 Theoretical developments

2.1 Statistical description of plate reverberation

Let us consider a propagation medium subject to an acoustic excitation caused by a single source emitting a signal $s_0(t)$. If the medium is unbounded, then the signal $s(r,t)$ received at a distance r away from the source may be characterised by its Fourier transform $\tilde{s}(r,\omega)$ expressed as:

$$\tilde{s}(r,\omega) = a(r)\, B(\omega)\, \tilde{s}_0(\omega)\, e^{-\gamma(\omega)\, r}\, e^{j\, k_d(\omega)\, r} \tag{1}$$

where $\tilde{s}_0$ is the Fourier transform of s_0, B is the frequency-dependent excitation amplitude, $k_d(\omega)$ is the dispersion law, $\gamma(\omega)$ is the attenuation law and $a(r)$ is the geometrical spreading term ($= 1/\sqrt{r}$ in the case of two-dimensional propagation).

If the medium is bounded and with low attenuation, then the signal $h_0(t)$ received at a given receiver R consists of the direct propagation signal $h_0^D(t) = s(r_0,t)$ from S to R, plus a reverberant part h_0^R corresponding to an infinite series of reflections on the medium boundaries:

$$h_0(t) = h_0^D(t) + h_0^R(t) \tag{2}$$

with

$$h_0^R(t) = \sum_{i=1}^{\infty} \kappa_i\, s(r_i,t) \tag{3}$$

where κ_i is the number of wavepackets coming from image-sources located at distances between r_i and $r_i + \Delta r_i$ from the receiver. If Δr_i is chosen small enough, then κ_i is either 1 or 0.

As explained in previous works [10], the contribution of the reflections can be conveniently described as a random Poisson process (shot-noise model) of characteristic parameter λ. Physically, $\lambda(r)$ can be interpreted as the average density of wavepackets propagated over the distance r. Hence, it is directly related to the expected value of κ_i in the following way:

$$E[\kappa_i] = \lambda(r_i)\, \Delta r_i \tag{4}$$

The expression of $\lambda(r)$ depends on the geometry of the reverberant propagation medium and can be conveniently determined using the image-source method. This will be illustrated here in the simple case of a rectangular-shaped medium subject to 2D-propagation (single-mode plate wave).

Let us consider a rectangular plate of surface $\mathcal{S}$ (represented by the solid lines in Fig. 1). The images of the primary source (emitter position) are located according to a periodic pattern, whose elementary cell is the dashed-line rectangle represented in Fig. 1 [9].

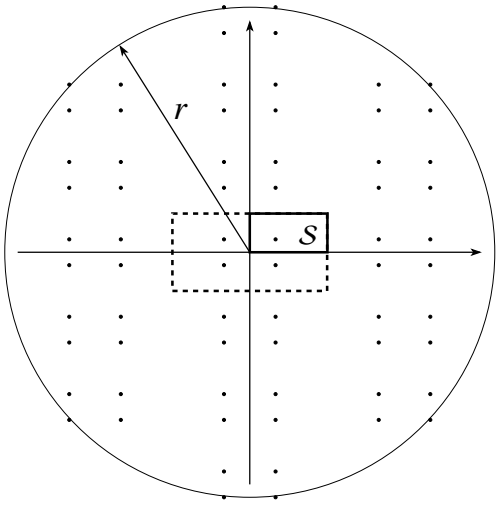

Figure 1: Image sources for a rectangular plate.

Each image source will generate its own wavepacket eventually arriving at the receiver. The ones located inside a disk of radius r will then produce wavepackets propagated over distances smaller than r. The number $\Lambda(r)$ of these image sources is four times the number of elementary cells included

in the disk. For r much greater than the plate dimensions, it corresponds approximately to the ratio of the disk surface and the plate surface:

$$\Lambda(r) \simeq \frac{\pi r^2}{\mathcal{S}} \tag{5}$$

Then, the number of wavepackets propagated over distances between r and $r + dr$ is $\Lambda(r + dr) - \Lambda(r) = d\Lambda$. The wavepacket density λ is thus defined as:

$$\lambda(r) = \frac{d\Lambda}{dr} \tag{6}$$

From Eq. (5), λ can then be estimated as:

$$\lambda(r) \simeq \beta_d\, r \tag{7}$$

with

$$\beta_d = \frac{2\pi}{\mathcal{S}} \tag{8}$$

For 2D-propagation case, the wavepacket density λ is thus a linear function of the propagation distance r. For structure shapes other than a rectangle, Eq. (7) still applies, but β_d would have an expression other than Eq. (8).

2.2 Derivation of the ensemble-averaged envelope

The envelope of $h_0^R(t)$ can be determined from the its complex analytic representation $H_0^R(t) = h_0^R(t) + j\hat{h}_0^R(t)$, where $\hat{\cdot}$ represents the Hilbert transform.

Then, from Eq. (3) the square of the envelope can be expressed as:

$$|H_0^R(t)|^2 = \sum_{i=1}^{\infty}\sum_{j=1}^{\infty} \kappa_i\kappa_j \left[s(r_i,t)\, s(r_j,t) + \hat{s}(r_i,t)\, \hat{s}(r_j,t) \right] \tag{9}$$

where $\hat{s}(r_i,t)$ is the Hilbert transform of $s(r_i,t)$.

Separating in the double sum above the terms with $i = j$ and the cross-terms, and taking the expected value then yields:

$$\begin{aligned} E\left[|H_0^R(t)|^2\right] = &\sum_i E[\kappa_i^2] \left[s^2(r_i,t) + \hat{s}^2(r_i,t) \right] \\ &+ \sum_i \sum_{j\neq i} E[\kappa_i\kappa_j] \left[s(r_i,t)\, s(r_j,t) \right. \\ &\left. + \hat{s}(r_i,t)\, \hat{s}(r_j,t) \right] \end{aligned} \tag{10}$$

Assuming that the random variables κ_i and κ_j are independent for $i \neq j$, remarking that $\kappa_i^2 = \kappa_i$ (since it is either 0 or 1) and invoking Eq. (4) the expected values in the equation above can be simplified to:

$$E[\kappa_i\kappa_j] = E[\kappa_i]E[\kappa_j] = \lambda(r_i)\,\lambda(r_j)\,\Delta r_i\,\Delta r_j \tag{11}$$

for $i \neq j$, and

$$E[\kappa_i^2] = E[\kappa_i] = \lambda(r_i)\,\Delta r_i \tag{12}$$

Replacing the discrete sums by integrals ($\Delta r_i \to dr, \Delta r_j \to dv$) then yields:

$$\begin{aligned} E\left[|H_0^R(t)|^2\right] = &\int_0^{+\infty} \lambda(r) \left[s^2(r,t) + \hat{s}^2(r,t) \right] dr \\ &+ \int_0^{+\infty}\int_0^{+\infty} \lambda(r)\lambda(v) \left[s(r,t)\, s(v,t) \right. \\ &\left. + \hat{s}(r,t)\, \hat{s}(v,t) \right] dr\, dv \end{aligned} \tag{13}$$

and thus

$$E\left[|H_0^R(t)|^2\right] = \int_0^{+\infty} \lambda(r)\, |S(r,t)|^2\, dr + \left| \int_0^{+\infty} \lambda(r)\, S(r,t)\, dr \right|^2 \tag{14}$$

We will make here the assumptions that the excitation signal s_0 is of finite duration T and with a narrow frequency band centered at ω_0, and that the attenuation coefficient $\gamma(\omega) \simeq \gamma_0$ is approximately constant in this frequency band. Note that if actually s_0 is not narrow-band then, simply, narrow-band filtering may be applied to the received signals.

First it can be shown that, in such conditions, the second integral in the relation above is zero (see [11]), meaning that the cross-terms contribution vanishes on average. Second, further developments (fully detailed in [11]) on the first integral lead to the following expression of the envelope:

$$E\left[|H_0^R(t)|^2\right] \simeq \lambda(r_t)\, a^2(r_t)\, D\, e^{-2t/\tau} \tag{15}$$

where

$$D = \int_0^{+\infty} v_g(\omega) \left| B(\omega)\, \tilde{S}_0(\omega) \right|^2 d\omega \tag{16}$$

with $\tau = 1/(\gamma_0 v_{g_0})$, $r_t = v_{g_0} t$, v_g is the group velocity and $v_{g_0} = v_g(\omega_0)$.

In the case of 2D-propagation, $a(r) = 1/\sqrt{r}$ and Eq. (7) yield:

$$E\left[|H_0^R(t)|^2\right] \simeq \beta_d\, D\, e^{-2t/\tau} \tag{17}$$

If v_g varies only slightly in the frequency band of the excitation, then

$$D \simeq v_{g_0}\, D_s \tag{18}$$

with

$$D_s = \int_0^{+\infty} \left| B(\omega_0)\, \tilde{S}_0(\omega) \right|^2 d\omega \tag{19}$$

This quantity corresponds to the acoustic power injected by the source into the medium.

As will be illustrated in Sec. 3.1, comparing the theoretical expression given in Eq. (17) to measured envelopes will allow identification of physical parameters.

2.3 Correlation functions and sensitivity to defect

In the same way, the statistical model described above can also be used to characterise the temporal correlation functions of two received signals. This could be particularly useful when the acoustic source emits a continuous noise instead of a signal of finite duration.

The cross-correlation of the signals $h_{1_0}(t)$ and $h_{2_0}(t)$ received respectively at two receivers in the defect-free state is notated $\varphi_{h_{1_0}h_{2_0}}$. Provided the autocorrelation $\varphi_0 = \varphi_{s_0s_0}$ of

the emitted signal s_0 is of finite duration $2T$ and of narrow frequency band centered at ω_0, a theoretical expression of $\varphi_{h_{1_0}h_{2_0}}(t)$ can be obtained [10]. For simplicity, this expression is given below for the case of a single receiver only (autocorrelation). Indeed, after the correlation peak (for $t \geq T$) the averaged squared autocorrelation corresponds to an exponentially decreasing function. With the additionnal simplifying assumptions of a constant excitation amplitude $B(\omega) = B_0$ and low dispersion, it can be expressed as:

$$E\left[\varphi^2_{h_0h_0}(t)\right] \simeq A_c\, e^{-2t/\tau} \tag{20}$$

with

$$A_c = B_0^4\,\Phi_0^2\left(\tau\, v_{g_0}^2\,\beta_d^2 + \frac{v_{g_0}\beta_d}{r_0}\right) e^{4r_0/v_{g_0}\tau} \tag{21}$$

where $\Phi_0^2 = \int_{-T}^{T}\varphi_0^2(t)\,dt$.

The correlation function $\varphi_{h_1h_2} = \varphi_{h_{1_0}h_{2_0}} + \Delta\varphi$ in the presence of a defect can be estimated following the same kind of process [10]. The sensitivity of the correlation function is then quantified through a "defect sensitivity parameter" defined as the ratio of the energy of $\Delta\varphi(t)$, directly related to the defect's presence, to the energy of $\varphi_{h_{1_0}h_{2_0}}(t)$, the defect-free correlation.

$$r_{12} = \frac{E\left[\int_{-\infty}^{\infty}\Delta\varphi^2(t)\,dt\right]}{E\left[\int_{-\infty}^{\infty}\varphi^2_{h_{1_0}h_{2_0}}(t)\,dt\right]} \tag{22}$$

For a defect characterised by a linear expression $\lambda_i'(t) = \gamma t + \varepsilon_i$ of the arrival time density of Δh_i and after complete derivation (detailed in [10]), the following expression is obtained:

$$r_{12} \simeq \alpha^2\left[\frac{P'_2}{Q'}\,e^{-2(\tau'_{0_1}-\tau_{0_1})/\tau} + \frac{P'_1}{Q'}\,e^{-2(\tau'_{0_2}-\tau_{0_2})/\tau}\right] + \alpha^4\,\frac{P'_3}{Q'}\,e^{-2(\tau'_{0_1}-\tau_{0_1}+\tau'_{0_2}-\tau_{0_2})/\tau} \tag{23}$$

This parameter is associated to the probability to detect a given defect. Its possible use will be illustrated below (see Sec. 3.2).

3 Possible applications

3.1 Passive parameter estimation

Eq. (17) shows that the expected envelope is characterized by a decreasing exponential fonction of the form:

$$E\left[|H_0^R(t)|^2\right] \simeq A\, e^{-2t/\tau} \tag{24}$$

with

$$A = v_{g_0}\,\beta_d\,D_s \tag{25}$$

The amplitude A is related both to structural characteristics of the medium and to source properties. Identification of the value of A from measured reverberant signals can then lead to interesting experimental characterisations.

This can be performed through a linear curve-fitting applied to the logarithm of the envelope averaged over a number of realisations. An illustration of this is given in Fig. 2, where numerical results obtained using a (deterministic) simulation based on the source-image method are compared to the theoretical expected envelope given by Eq. (24). The considered propagation medium is a 6-mm thick rectangular aluminum plate with lateral dimensions 2×1 m^2. The signal s_0 emitted by the source is a five-cycle Hann-windowed sinusoid waveform with central frequency $f_0 = \omega_0/2\pi = 15$ kHz. The envelope of the simulated signal received by a single receiver is shown in thin dotted blue line in Fig. 2-(a), whereas the averaged envelope over five different sensor positions is represented in Fig. 2-(b). Logically, the second (averaged) curve is closer to the theoretical expectation of the envelope shown in thick red solid-line in both figures. A simple curve-fitting applied to this one allows a very good retrieval of the parameters A and τ of the theoretical curve (see the green dashed line in Fig. 2-b).

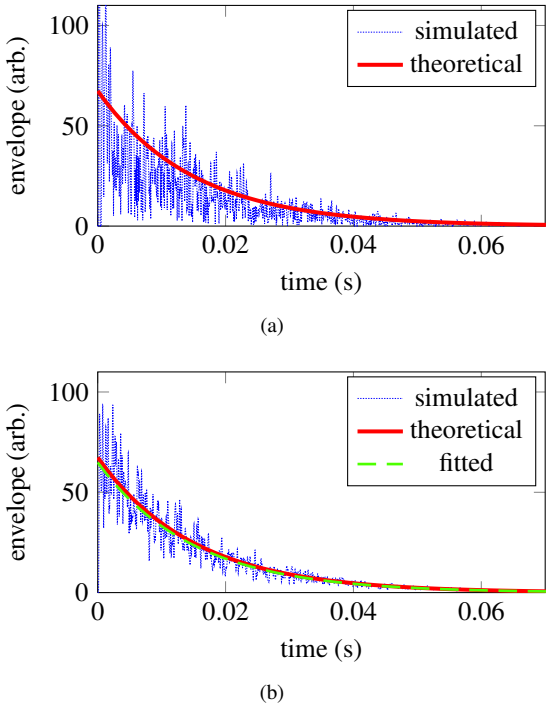

Figure 2: Simulated result and comparison to theoretical and estimated envelopes. (a) Envelope at 1 sensor position. (b) Average envelope over 5 sensor positions.

In an experimental point of view, it might not be always possible or convenient to get different realisations of received signals. Therefore it would be interesting to make the parameter identification work even on a single signal. In such case, it can be judicious to apply an integration-based technique similar to the so-called Schroeder method [12], well known in architectural acoustics. Instead of working directly on a received signal $h_0^R(t)$ or its envelope, we define the function $I_s(t) = \int_t^{+\infty}[h_0^R(u)]^2\,du$, which can be computed numerically.

Departing from Eq. (3), it can be theoretically shown that I_s is also a decreasing exponential function:

$$I_s(t) \simeq \frac{A\tau}{4}\,e^{-2t/\tau} \tag{26}$$

where A is as defined in Eq. (25).

An example of application of this "Schroeder-like" method is shown in Fig. 3. The integral function $I_s(t)$ is computed from the simulated received signal (blue dashed line) and compared to the theoretical curve (red solid line) given by Eq. (26). Apart from the early-time behaviour, which is erroneously described by the statistical model, the agreement

between both curves is very good even though a single realisation only is used. This remarkable behaviour means that the time integration replaces here in some way an average over different realisations, which is something like an ergodicity property. Obviously in that case, curve-fitting will also provide results of good quality.

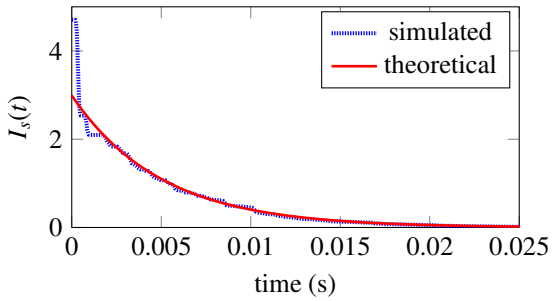

Figure 3: Simulated result and comparison to theoretical and estimated curves $I_s(t)$ for a single receiver (Schroeder-like method).

In summary, by applying either the curve-fitting process to the averaged envelopes (when several realisations are available) or the Schroeder-like method to a single received signal, an accurate estimation of the value of A may be obtained. However, in order to be able to deduce structural characteristics, the effective acoustic power D_s injected by the source into the medium in the considered frequency band has to be known. Since this is highly improbable in practice, an equation will be missing to solve the problem.

What is proposed here is then to relate these source properties to the early (deterministic) part of the received signals. If the first (direct) wavepacket is temporally separated from the higher order ones (which is the case when the source-receiver distance is small compared to the structure's characteristic dimensions), then a simple relationship between D_s and the energy I_0^D of this wavepacket (defined below) can be used as the missing equation.

$$I_0^D = \int_{\tau_0}^{\tau_0+T} \left|H_0^D(t)\right|^2 \, dt \tag{27}$$

Indeed, applying the Parseval's theorem, it can be easily shown [11] that:

$$I_0^D \simeq \frac{D_s}{r_0} \tag{28}$$

where r_0 is the source-receiver distance.

Thus, Eq. (25) and (28) constitute together the basis of an original parameter extraction principle. Depending on the experimental situation considered, the value of one of the three physical parameters v_{g_0}, β_d or r_0 can be estimated, in addition to the acoustic power D_s emitted in the frequency band. The corresponding relationships are given below:

1. If r_0 and v_{g_0} are known, then:

$$\begin{cases} D_s \simeq r_0 \, I_0^D \\ \beta_d \simeq \dfrac{A}{r_0 \, v_{g_0} \, I_0^D} \end{cases} \tag{29}$$

which allows an estimation of the medium dimensions (plate surface, see Eq. 8 for the particular case of a rectangular plate).

2. In the same way, if r_0 and β_d are known, then:

$$\begin{cases} D_s \simeq r_0 \, I_0^D \\ v_{g_0} \simeq \dfrac{A}{r_0 \beta_d \, I_0^D} \end{cases} \tag{30}$$

which constitutes an estimation of the propagation velocity without any time measurement.

3. And finally, if v_{g_0} and β_d are known, then:

$$\begin{cases} D_s \simeq \dfrac{A}{v_{g_0} \beta_d} \\ r_0 \simeq \dfrac{A}{v_{g_0} \beta_d \, I_0^D} \end{cases} \tag{31}$$

which allows to estimate the source-receiver distance without time measurement and synchronization.

The third case is illustrated by promising experimental results. A rectangular plate with the same characteristics as in the simulations presented above has been used. The acoustic excitation is provided through a pencil lead break manually applied to the plate surface. The structural properties of the plate being known, the values of v_{g_0} and β_d are easily accessible. The method presented above has been applied to the signal received at a single piezoelectric receiver, after band-pass filtering by a convolution with a five-cycle Hann-windowed sinusoid waveform with adjustable central frequency f_0 between 15 and 30 kHz. The receiver is separated from the source by a distance $r_0 = 10$ cm. As shown in Fig. 4, the application of Eq. (31) provides a fairly good estimation of the value of r_0 (green circles) in the whole frequency range. Averaging over the values obtained for every frequency in the range gives $r_{0_{\text{moy}}} = 9.5$ cm, which is not bad at all when considering the ill-calibrated excitation method and the absence of time synchronisation between source and receiver.

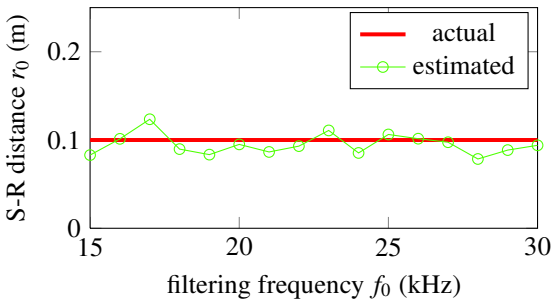

Figure 4: Estimation of r_0 from the measured impulse response.

In the case of a source emitting a continuous noise, the received signals do not exhibit the exponential decrease characteristic of the reverberant properties of the medium. In that case, it is interesting to note that the curve-fitting process presented above can be similarly applied to the squared correlation functions, as suggested by the form of Eq. (20). Like for A, the identified value of A_c is then related to both structural and source parameters (Eq. 21).

3.2 Defect detection from noise correlation

To illustrate the capabilities of the correlation functions for defect detection on a practical case, we consider two sensors R_1 and R_2 and a source S located at given (fixed) positions of the plate. The sensitivity of the auto- or cross-correlation to a defect of coordinates (x, y) can be theoretically estimated using Eq. (23). Then, by representing the value of r or r_{12} in color level for each (x, y) on the discretized plate surface (2D-grid), a map of the sensitivity to the defect can be established for the particular measurement configuration.

In Fig. 5, the sensitivity of the autocorrelation of the signal on a single receiver is characterised for two different source-receiver distances. The source and receiver positions are represented by a cross (+) symbol and a circle (o), respectively.

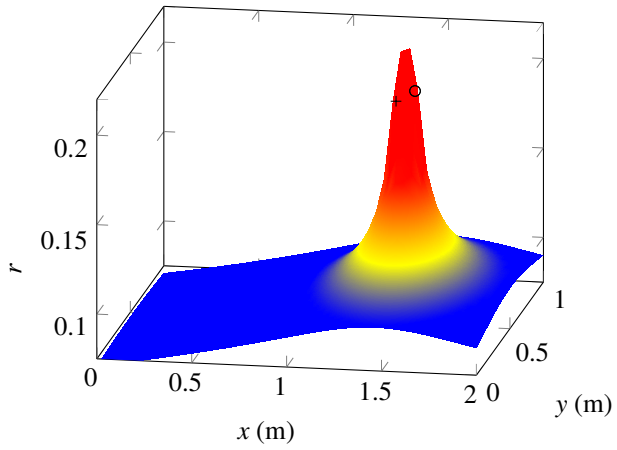

(a)

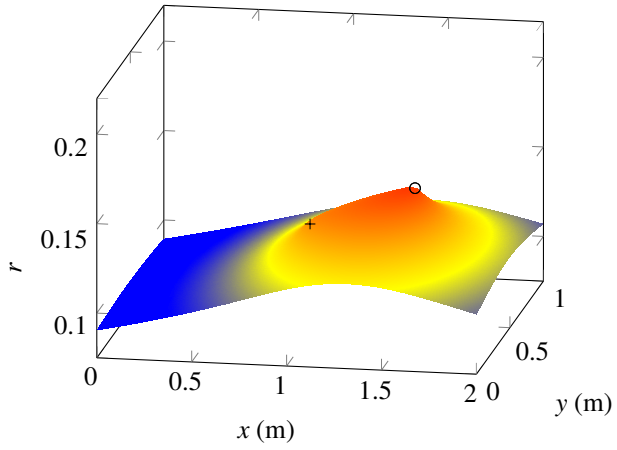

(b)

Figure 5: Dependance of the sensitivity parameter r on the defect position

What can be clearly observed from these results is that the defect detection capability is strongly related to the relative positions of the source, the receiver(s) and the defect. The obvious peak in Fig. 5-(a) shows that when the source and the receiver are close to each other, the sensitivity of the correlation function to the defect is very strong inside a small area around them and rapidly decreases as the defect position gets farther. Fig. 5-(b), corresponding to a larger source-receiver distance, exhibits a larger defect detection area, but with a lower probability of detection.

Fig. 6 shows that using two receivers and working on the cross-correlation function basically leads to the same kind of

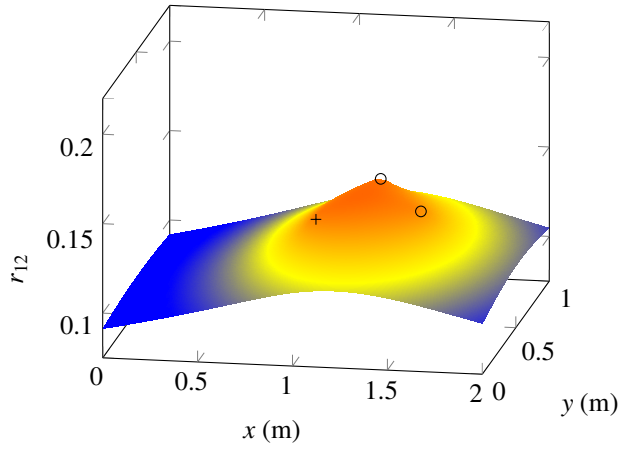

(a)

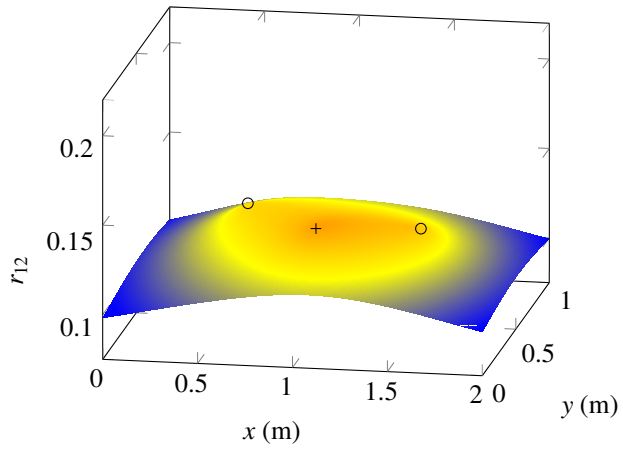

(b)

Figure 6: Dependance of the sensitivity parameter r_{12} on the defect position

results. The additional benefit here is that positioning both receivers farther from each other (see Fig. 6-b) has the effect of extending the potential detection area, independently of the source location. Here again, the counterpart is naturally a lower sensitivity to the defect and thus detection probability.

Note that in the context of a sensor network covering the whole medium area, this effect could be compensated by the multiplication of sensors.

4 Conclusion

The results presented in this paper illustrate the possibility of extracting quantitative information from a minimal number of sensors by exploiting the statistical properties of the acoustic reverberation in a solid plate. First, using the theoretical relationship between the statistical characteristics of the envelope of the impulse response and the structural and source properties, it has been shown how parameter estimation could be achieved by associating fitted features to "ballistic" wave data. Second, the average influence of a localized defect on the correlation functions has been derived as a function of a limited number of parameters: the reverberation properties of the medium, the radiation characteristics of the damage and the relative positions of the source, the receiver and the defect. Then, the possible detection of the defect for a given source and receivers setup has been discussed.

Future work will focus on developing further this idea of combining the late and early properties of the impulse response or, in the case of a continuous noise, of the correlation functions. Taking into account not only the first, but several early reflections should increase the application potential of the method.

References

[1] A. Derode, A. Tourin, and M. Fink. Ultrasonic pulse compression with one-bit time reversal through multiple scattering. *J. Appl. Phys.*, 85:6343–6352, 1999.

[2] A. Aubry and A. Derode. Detection and imaging in a random medium: A matrix method to overcome multiple scattering and aberration. *J. Appl. Phys.*, 106:044903, 2009.

[3] E. Larose, A. Derode, M. Campillo, and M. Fink. Imaging from one-bit correlations of wideband diffuse wave fields. *J. Appl. Phys.*, 95:8393, 2004.

[4] E. Larose, T. Planes, V. Rossetto, and L. Margerin. Locating a small change in a multiple scattering environment. *Appl. Phys. Lett.*, 96:204101, 2010.

[5] E. Moulin, N. Abou Leyla, J. Assaad, and S. Grondel. Applicability of acoustic noise correlation to Structural Health Monitoring in non-diffuse field conditions. *Appl. Phys. Lett.*, 95:094104, 2009.

[6] A. Duroux, K. G. Sabra, J. Ayers, and M. Ruzzene. Using cross-correlations of elastic diffuse fields for attenuation tomography of structural damage. *J. Acoust. Soc. Am.*, 127:3311–3314, 2010.

[7] J. de Rosny, P. Roux, M. Fink, and J. H. Page. Field fluctuation spectroscopy in a reverberant cavity with moving scatterers. *Phys. Rev. Lett.*, 90:094302, 2003.

[8] J. E. Michaels, Y. Lu, and T. E. Michaels. Methodologies for quantifying changes in diffuse ultrasonic signals with applications to structural health monitoring. In *Proc. SPIE*, volume 5768, pages 97–105. T. Kundu, 2005.

[9] J. Cuenca, F. Gautier, and L. Simon. The image source method for calculating the vibrations of simply supported convex polygonal plates. *J. Sound Vib.*, 322:1048–1069, 2009.

[10] N. Abou Leyla, E. Moulin, and J. Assaad. Influence of a localized defect on acoustic field correlation in a reverberant medium. *J. Appl. Phys.*, 110:084906, 2011.

[11] E. Moulin, H. Achdjian, J. Assaad, N. Abou Leyla, K. Hourany, and Y. Zaatar. Extraction of the statistical properties of the impulse response of a reverberant plate and application to parameter estimation. *J. Acoust. Soc. Am.*, submitted for publication, 2012.

[12] M. R. Schroeder. New Method of Measuring Reverberation Time. *J. Acoust. Soc. Am.*, 37:409–412, 1965.